



Self-elongated growth of nanopores in annealed amorphous Ta₂O₅ films

著者	Nakamura R., Tanaka K., Ishimaru M., Sato K., Konno T.J., Nakajima H.
journal or publication title	Scripta Materialia
volume	6
number	3-4
page range	182-185
year	2012-02
権利	(C) 2012 Acta Materialia Inc. Published by Elsevier Ltd. NOTICE: this is the author's version of a work that was accepted for publication in Scripta materialia. Changes resulting from the publishing process, such as peer review, editing, corrections, structural formatting, and other quality control mechanisms may not be reflected in this document. Changes may have been made to this work since it was submitted for publication. A definitive version was subsequently published in Scripta materialia, 66, 3-4, 2012. doi:10.1016/j.scriptamat.2011.10.033
URL	http://hdl.handle.net/10466/15020

doi: 10.1016/j.scriptamat.2011.10.033

Self-elongated growth of nanopores in annealed amorphous Ta₂O₅ films

R. Nakamura^{a,*}, K. Tanaka^a, M. Ishimaru^a, K. Sato^b, T.J. Konno^b, H. Nakajima^a

^a*The Institute of Scientific and Industrial Research, Osaka University, Mihogaoka 8-1, Ibaraki, Osaka 567-0047, Japan*

^b*Institute for Materials Research, Tohoku University, Katahira 2-1-1, Sendai 980-8577, Japan*

Nanoporous β -Ta₂O₅ films with oriented and elongated nanopores have been prepared by a technique which utilizes the accumulation of free volume during the crystallization of amorphous Ta₂O₅ annealed above 973 K. The TEM analyses revealed that voids were elongated in the [100] direction perpendicular to the longitudinal b axis of the orthorhombic structure. The self-assembly of a significant amount of oriented nanovoids can be contributed to the strong anisotropic crystal structure of orthorhombic Ta₂O₅.

KEYWORDS: Nanoporous; Oxides; Amorphous; Crystallization, Self-assembly

*Corresponding author. Tel. :+81 6 6879 8437; fax: +81 6 6879 8439; e-mail: rnakamur@sanken.osaka-u.ac.jp

Tantalum oxides have received considerable attention as protective coating materials for chemical equipment, in optical devices and are considered suitable material for storage capacitors in very large-scale integrated circuits.¹⁻⁵ Since it has excellent dielectric properties, the ability to fabricate nanoporous Ta₂O₅ films with a high specific charge by controlling the nanostructures of Ta₂O₅ would mean much wider applications in electronics and in sensor devices.⁶ Typically, nanoporous oxide materials can be achieved by chemical synthesis routes, sintering nanopowders and clustering implanted gas-bubbles⁷. For example, it is known that nanoporous Ta₂O₅ layers can be obtained on the metallic Ta surfaces^{6,8} via electrochemical anodization^{9,10}. At present, however, the methods to obtain nanoporous Ta₂O₅ are limited to the electrochemical anodization.

Recently, a different process for the preparation of nanoporous oxides has been proposed by our group. Amorphous Al₂O₃ and WO₃ have been found to become nanoporous structures as a result of crystallization.¹¹ The formation and growth of high density nanopores can be explained by the accumulation of atomic spaces, i.e., free volumes, which are considered to be essentially included in amorphous Al₂O₃ and WO₃ with 20-30 % lower density than their crystalline phases. Since amorphous Ta₂O₅ is also known to be much less dense than its crystalline phase (β -Ta₂O₅),^{13,14} it is reasonable to expect nanoporous Ta₂O₅ can be obtained by annealing an amorphous Ta₂O₅ film.

The present work investigates the possibility of forming nanoporous structures via the annealing of amorphous Ta₂O₅. The growth of self-organized unidirectional nanopores as a result of crystallization was examined by transmission electron microscopy (TEM).

The thin films of amorphous Ta₂O₅ were prepared by sputtering a Ta₂O₅ target (99.9%) at a radio-frequency of 150 Hz under an Ar pressure of 1.0 Pa. A cleavage NaCl crystal was used as the substrate. The substrate was cooled via a liquid nitrogen reservoir and kept at 100 K. The NaCl on which the 15~30 nm thick oxide thin film was deposited was put into distilled water, and then the floating thin film was mounted onto a Pt grid. The amorphous oxide on the Pt grid was subjected to heat-treatment in an electric furnace in air at 773~1123 K for 3.6 ks. The changes in its morphology and structure were examined by a Hitachi H-800 type TEM operated at 200 kV. The structure of the crystallized oxides was analyzed by a JEOL JEM-3000F TEM at 300 kV. Atomic number contrast (Z-contrast) images of scanning TEM (STEM) were obtained using a FEI Titan 80-300 TEM operating at 300 kV with a high-angle annular dark-field (HAADF) detector. The tilt series of Z-contrast images were acquired within the detector angle between 60 and 210 mrad and 3D reconstruction was performed by using the INSPECT3D software package (FEI Co. Ltd).

Figure 1 shows the bright-field images (BFIs) of as-deposited (a) and annealed (b-e) Ta₂O₅ at 773-973 K, together with the corresponding selected electron diffraction patterns. As shown in Fig. 1(a), no void contrast can be detected in an as-deposited thin film of amorphous Ta₂O₅. On the other hand, the high density of spherical nanovoids with an average diameter of between 2.3 and 3.5 nm is clear in amorphous Ta₂O₅ annealed above 773 K. The structure of the thin film remains amorphous up to 923 K at an annealing time of 3.6 ks. At 973 K, crystallized regions appear in the amorphous matrix, as can be seen in Fig. 1(e). In the amorphous region, a number of spherical nanovoids can be seen as is the case with at 873 K (c) and 923 K (d). On the other hand, voids in the crystallized region grow larger than those in the amorphous region. It is particularly noteworthy that the voids near the front of interface of the crystalline phase tend to be elongated, whereas voids in the center of it are spherical. In the early stages of crystal growth, a crystallite has a variety of different facets which develop at random. As the crystallite grows, the faster growing facets are annihilated and slower ones develop. Fig. 1(e) represents the shape of the facet due to the development of slower growing planes. It seems, therefore, that the elongated voids at the front of the interface originate in the preferential growth of a specific plane.

Figure 2 shows the changes in the average void diameter, d , and the areal fraction of voids, S , obtained by an image analysis of the amorphous region of Ta₂O₅ after annealing at 773-973 K. The value of d is considered equivalent to the diameter, assuming the voids are spherical, and S is determined by dividing the sum of the occupied areas voids occupy by the area on the TEM image.

Both d and S tend to increase with increasing annealing temperature although S is saturated at 923 K, indicating that the formation of new voids and the growth of the existing voids take place before crystallization. It should be noted that the void formation behavior in annealed amorphous Ta₂O₅ is different from that in annealed amorphous Al₂O₃ and WO₃, where no increase in void size is observed before crystallization.¹² The growth of nanovoids in the amorphous region suggests that amorphous Ta₂O₅ intrinsically contains a significant amount of free volume, and free volume is considered to be the prerequisite for the formation and growth of nanovoids.

Figure 3 shows the BFIs and electron diffraction patterns of fully crystallized Ta₂O₅ films after annealing at 1023 K for 3.6 ks, where an array of elongated nanopores appears. The voids after full crystallization at 1023 K became faceted compared to those of the crystallized region in the amorphous matrix at 973 K (Fig. 1(e)). The structure of crystallized Ta₂O₅ was identified as the low temperature phase, commonly referred to as orthorhombic β -Ta₂O₅ ($a=0.389$ nm, $b=4.029$ nm, $c=0.620$ nm¹⁵). The simulated electron diffraction patterns for the orthorhombic structure are in agreement with the experimentally obtained diffraction patterns. In both areas, the longitudinal direction of voids is parallel to the a axis and perpendicular to the longitudinal b axis of the orthorhombic structures. The reconstructed 3D image of Ta₂O₅ after annealing at 1023 K, shown in Fig. 4, reveals that rather than being tabular in shape, the voids in orthorhombic β -Ta₂O₅ are columnar, indicating the preferential growth of nanovoids toward a direction of [100].

It is known that the shape of voids is determined either by thermodynamic or by kinetic factors: the former is based on the achievement of the lowest free energy which the system including voids of a particular shape has and the latter refers to how the various growth processes, such as step nucleation and surface diffusion, affect the development of a specific shape.¹⁶ In the case of the crystallization of amorphous Ta₂O₅, the void growth goes along with the crystal growth, indicating that the predominating contributors to the morphology of the nanovoids are the kinetic factors. As shown in Figs. 2 and 3, nanovoids become elongated perpendicular to the slower growing (100) plane. Therefore, the slow crystal growth of the (100) plane is closely related to the self-assembly of the elongated nanovoids towards [100] direction. The growth of the (100) plane of β -Ta₂O₅ in the amorphous matrix is controlled by the nucleation of the (010) faceted steps and their propagation along [010] on the (100) plane.¹⁷ One possible reason for the slow growth of the (100) plane may be the long periodic structure of the β -Ta₂O₅ unit along the b -axis direction; the atomic arrangement towards the long-periodic b -axis in the (100) plane is more difficult than the a - and c -axes. The strong isotropic nature of β -Ta₂O₅ allows for the faceted growth of (001) plane, which provides the growing nanovoids with enough time to absorb free volume as well as existing nanovoids at the boundary between amorphous and crystalline phases as crystal growth occurs.

In an earlier paper,¹² we proposed that nanovoid formation in the crystallization process of amorphous Al₂O₃ and WO₃ is due to the accumulation of a large amount of free volumes in the

amorphous oxides which are characteristically 20~30% less dense than the crystalline phases. Since the formation and growth of nanovoids in amorphous Ta₂O₅ take place during the structural change toward β -Ta₂O₅, as they do with amorphous Al₂O₃ and WO₃, this can be considered true of amorphous Ta₂O₅. However, two peculiar behaviors were noted in the void formation and growth in the annealed Ta₂O₅. One is the void formation and growth behavior in the amorphous region. The diameter of the voids continues to increase with increasing annealing temperature (Fig. 2). This tendency was not seen in amorphous Al₂O₃ or WO₃, where the diameter of the voids remained constant before crystallization. It can therefore be assumed that amorphous Ta₂O₅ intrinsically contains a large amount of free volume, which is the source of void formation and growth. The other is the oriented and elongated growth of the voids due to crystallization. This self-assembly of oriented nanovoids can be attributed to the strong anisotropic crystal structure of orthorhombic Ta₂O₅. In the process of crystal growth, the void growth takes place via the coalescence of voids. When amorphous oxides contain a large amount of free volume and the crystalline phases are composed of a strong anisotropic unit cell, it can be concluded that the crystallization of amorphous oxides induces the self-oriented growth of nanopores.

In conclusion, oriented and elongated nanoporous structures of β -Ta₂O₅ have been fabricated through a simple heat-treatment process of amorphous Ta₂O₅. The formation of the self-organized nanostructure can be attributed to the strong anisotropy of β -Ta₂O₅. The fabrication of such porous nanostructures with such a highly controlled morphology will enable the application of Ta₂O₅ to expand considerably. Therefore, further research on how to control the growth of nanovoids associated with crystal growth is required to show both the possibilities and limits for the use of the nanoporous β -Ta₂O₅ prepared by this technique in new applications.

The authors would like to thank for supporting the TEM observations by the Research Center for Ultra-High Voltage Electron Microscopy and the Comprehensive Analysis Center of ISIR, Osaka University. A portion of this study was performed under the inter-university cooperative research program of the IMR, Tohoku University. This work was supported by Priority Assistance for the Formation of World Wide Renowned Centers of Research - The Global COE Program (Project: Center of Excellence for Advanced Structural and Functional Materials Design), from the Ministry of Education, Culture, Sports, Science and Technology, Japan.

- [1] C. Chaneliere, J. L. Autran, R. A. B. Devine, B. Balland, *Mater. Sci. Eng. R* 22 (1998) 269.
- [2] Y. Nishioka, S. I. Kimura, H. Shinriki, K. Mukai, *J. Electrochem. Soc.* 134 (1987) 410.
- [3] A. I. Kingon, J.-P. Maria, S. K. Streiffer, *Nature* 406 (2000) 1032.
- [4] R. S. Devan, S.-Y. Gao, W.-D. Ho, J.-H. Lin, Y.-R. Ma, P. S. Patil, Y. Liou, *Appl. Phys. Lett.* 98 (2011) 133117.
- [5] D. A. Deen, D. F. Storm, R. Bass, D. J. Meyer, D. S. Katzer, S. C. Binari, J. W. Lacin, T. Gougousi, *Appl. Phys. Lett.* 98 (2011) 023506.
- [6] I. Sieber, B. Kannan, P. Schmuki, *Electrochem. Solid-State Lett.* 8 (2005) J10.
- [7] B. J. Kooi, J. T. M. De Hosson, H. Schut, A. V. Fedorov, F. Labohm, *Appl. Phys. Lett.* 76 (2000)1110.
- [8] K. Kamada, M. Mukai, Y. Matsumoto, *Electrochim. Acta* 49 (2004) 321.
- [9] H. Masuda, K. Fukuda, *Science* 268 (1995) 1466.
- [10] H. Tsuchiya, J. M. Macak, I. Sieber, P. Schmuki, *Small* 1 (2005) 722.
- [11] R. Nakamura, T. Shudo, A. Hirata, M. Ishimaru, H. Nakajima, *Scr. Mater.* 64 (2011) 197.
- [12] D. Lüzenkirchen-Hecht, R. Frahm, *Physica B* 283 (2000) 108.
- [13] R. Bassiri, K. B. Borisenko, D. J. H. Cockayne, J. Hough, I. MacLaren, S. Rowan, *Appl. Phys. Lett.* 98 (2011) 031904.
- [14] R. S. Roth, J. L. Waring, H. S. Parker, *J. Solid State Chem.* 2 (1970) 445.
- [15] P. J. Goodhew, *Metal Sci.* 15 (1981) 377.
- [16] P. J. Beckage, D. B. Knorr, X. M. Wu, T. M. Lu, E. J. Rymaszewski, *J. Mater. Sci.* 33 (1998) 4375.

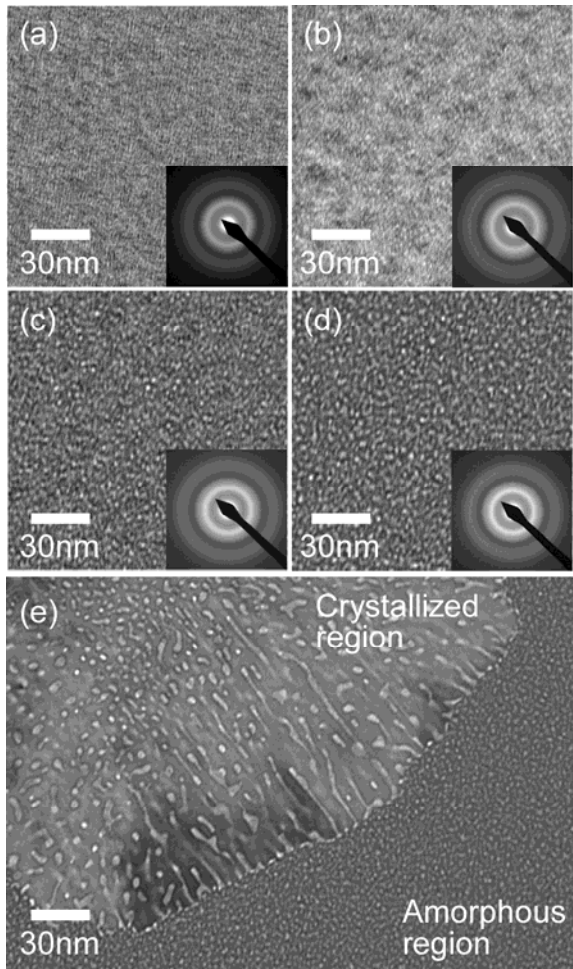


Figure 1. Bright field images and their corresponding selected-area electron diffraction patterns of as-deposited (a) and annealed (b-e) amorphous Ta_2O_5 . (b) 773 K, (c) 873 K, (d) 923 K, and (e) 973 K for 3.6 ks.

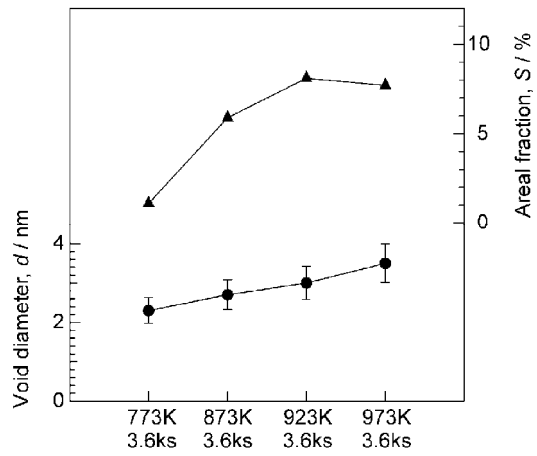


Figure 2. Changes in void diameter, d (solid circle), and areal fraction, S (solid triangle), in the annealed amorphous states.

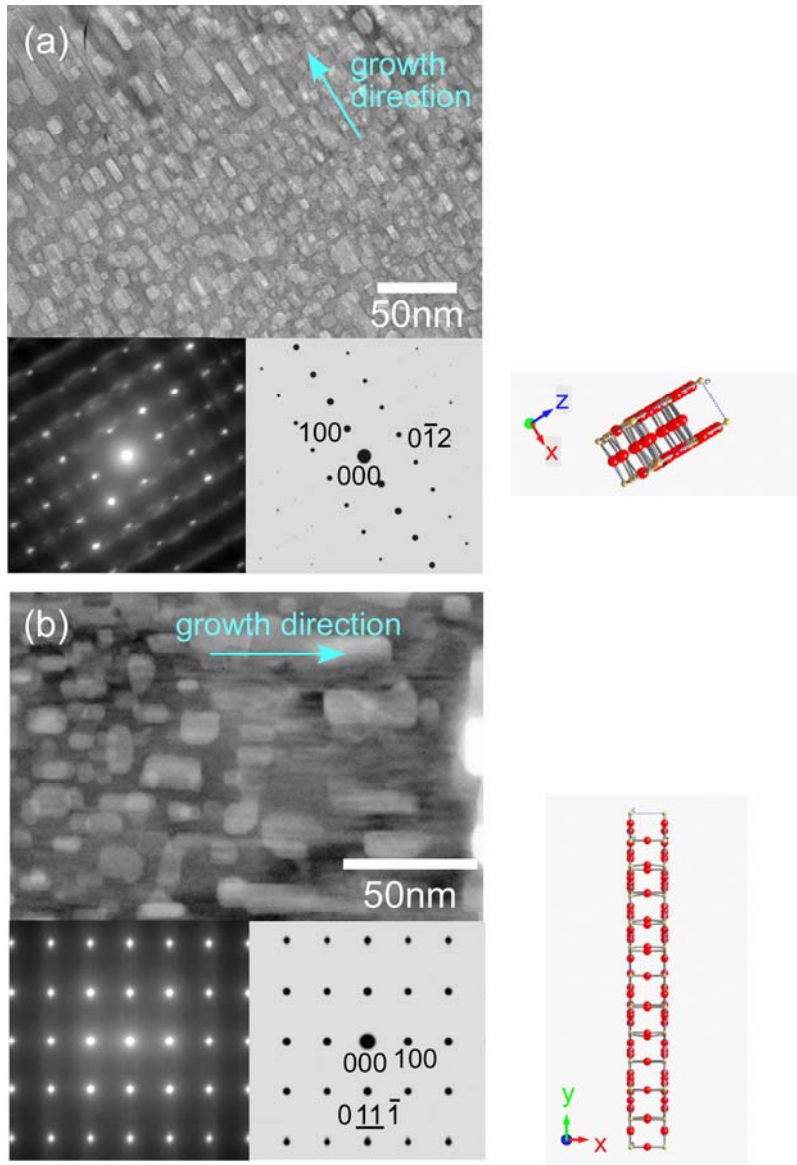


Figure 3. BFIs and electron diffraction patterns for the areas of the fully crystallized Ta_2O_5 films with different crystal orientations after annealing at 1023 K for 3.6 ks. b and c axes are perpendicular to the photographs in the (a) and (b) regions, respectively. Simulated diffraction patterns are shown together.

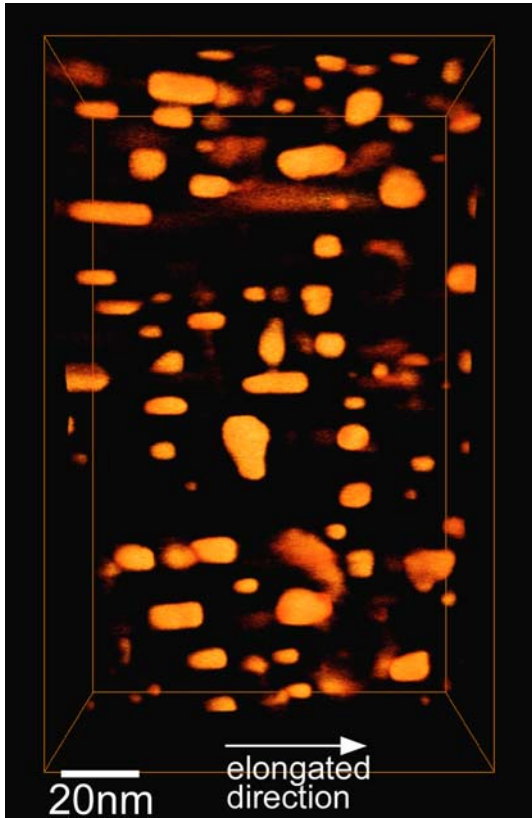


Figure 4. A reconstructed 3D image of elongated nanovoids included in the crystallized Ta₂O₅ at 1023 K for 3.6 ks observed by HAADF-STEM tomography.